



저작자표시-비영리-변경금지 2.0 대한민국

이용자는 아래의 조건을 따르는 경우에 한하여 자유롭게

- 이 저작물을 복제, 배포, 전송, 전시, 공연 및 방송할 수 있습니다.

다음과 같은 조건을 따라야 합니다:



저작자표시. 귀하는 원저작자를 표시하여야 합니다.



비영리. 귀하는 이 저작물을 영리 목적으로 이용할 수 없습니다.



변경금지. 귀하는 이 저작물을 개작, 변형 또는 가공할 수 없습니다.

- 귀하는, 이 저작물의 재이용이나 배포의 경우, 이 저작물에 적용된 이용허락조건을 명확하게 나타내어야 합니다.
- 저작권자로부터 별도의 허가를 받으면 이러한 조건들은 적용되지 않습니다.

저작권법에 따른 이용자의 권리는 위의 내용에 의하여 영향을 받지 않습니다.

이것은 [이용허락규약\(Legal Code\)](#)을 이해하기 쉽게 요약한 것입니다.

[Disclaimer](#)

공학석사학위논문

**Experimental Study about Effect of
the Flow rate on Combustion Instability
in Partially Premixed Gas Turbine Combustor**

**부분 예혼합 가스터빈 연소기에서의
연료 및 공기 유량에 따른 연소불안정
특성에 관한 실험적 연구**

2019 년 02 월

서울대학교 대학원

기계항공공학부

곽 상 혁

Abstract

Experimental study about effect of the flow rate on combustion instability in partially premixed gas turbine combustor

Sanghyeok Kwak

School of Mechanical and Aerospace Engineering

The Graduate School

Seoul National University

Recently, as concerns about environmental issues are emerging, much effort is being made to reduce the exhaust gases like NO, CO in the gas turbine industry. The most commonly used method is lean premixed combustion, which means that the combustion is occurring under oxidizer rich condition. The lean premixed combustion can reduce the exhaust gases, but there are disadvantages that the combustion instabilities, which affect reliability of the engine, is liable to occur. So, many of the studies about the combustion instability in the gas turbine is in progress.

In this study, effects of the fuel and air flow rate on the combustion instability in a partially premixed gas turbine combustor was investigated using laser diagnostics techniques like OH planar laser chemiluminescence (OH-PLIF) and particle image velocimetry (PIV). When large-scale change of the flow rate occurred, frequency of the combustion instability changed from low frequency to high frequency. To explain this phenomenon, convective delay time, defined as the distance from nozzle to flame divided by exit velocity of the fuel-air mixture at the nozzle, was introduced. Under various equivalence ratio and mean injection velocity conditions, the relationship between the change of the instability frequency and the change of the convective delay time was investigated. In addition, the effect of the small-scale change of the flow rate was examined. When the combustion instability occurs, the pressure fluctuations in the combustor induce the small-scale change of the air and fuel flow rate in the nozzle. The changes of the injection velocity of the fuel and air due to the changes of the flow rate lead to variation of the fuel-air mixing ratio due to change of momentum ratio in jet in cross-flow. So this cyclic variation of the fuel-air mixing ratio made periodic alternation of the length of the unburned mixture which is composed of unburned fuel and air mixture in unstable flames. Furthermore, in partially premixed flames, the flame had longer delay time between pressure and

heat release rate due to delay time for fuel and air mixing than the fully premixed flame. So, the partially premixed flame had lower instability frequency than the fully premixed flame. And it was also confirmed that the partially premixed flame had a more V-shaped flame structure than the fully premixed flame due to the more fluctuating delay time owing to the variation of the fuel-air mixing ratio.

Keywords: Gas turbine combustor, Combustion instability, Flame structure, Instability frequency shifting

Student number : 2017-28315

Contents

Chapter 1	INTRODUCTION.....	1
1.1	Combustion instability.....	1
1.2	OH chemiluminescence	3
1.3	OH planar laser induced fluorescence (OH-PLIF)	6
1.4	Particle image velocimetry (PIV)	8
1.5	Overview of present works	10
Chapter 2	APPARATUS AND EXPERIMENTAL METHOD	
	13
2.1	Model gas turbine combustor.....	13
2.2	Diagnostics setup.....	16
2.2.1	Setup for OH chemiluminescence	17
2.2.2	Setup for OH-PLIF	18
2.2.3	Setup for PIV	19
2.3	Test condition.....	21
Chapter 3	RESULTS AND DISCUSSION.....	24

3.1	The effect of the large-scale variation.....	24
3.2	The effect of the small-scale variation.....	37
Chapter 4 CONCLUSION.....		49
Bibliography.....		52
Abstract in Korean		54

List of Tables

Table 1.1	Typical radicals from hydrocarbon fuel combustion process.....	5
Table 1.2	Formation and destruction processes of OH radical.....	7
Table 2.1	Experimental conditions	22

List of Figures

Fig 1.1	Two burner assemblies, left : intact , right : damaged due to instability	2
Fig 1.2	Feedback loop of the combustion instability.....	2
Fig 1.3	Spectrum of chemiluminescence light from typical flames	5
Fig 1.4	Principle of typical PIV system	9
Fig 2.1	Schematic of test facility	13
Fig 2.2	Schematic of partially premixed type swirler	14
Fig 2.3	Schematic of model gas turbine combustor	14
Fig 2.4	Region of interest of each measurement techniques.....	16
Fig 2.5	High speed CMOS camera, intensifier and programmable timing unit	17
Fig 2.6	Optical setup for OH-PLIF measurement	18
Fig 2.7	Optical setup for PIV measurement	19

Fig 3.1	Instability frequency change increasing fuel flow rate (air = 1100 slpm)	24
Fig 3.2	Direct flame images and averaged OH-PLIF images increasing fuel flow rate (air = 1100 slpm)	25
Fig 3.3	Injection velocity change increasing fuel flow rate (air = 1100 slpm)	27
Fig 3.4	Instability frequency change decreasing air flow rate (fuel = 69 slpm)	29
Fig 3.5	Direct flame images and averaged OH-PLIF images decreasing air flow rate (fuel = 69 slpm)	30
Fig 3.6	Injection velocity change decreasing air flow rate (fuel = 69 slpm)	31
Fig 3.7	Instability frequency change increasing air flow rate under constant equivalence ratio	32
Fig 3.8	Direct flame images increasing flow rate under constant equivalence ratio	34
Fig 3.9	Injection velocity change increasing air flow rate under constant equivalence ratio	35

Fig 3.10	Mode analysis about instability of 500 Hz (a) FFT result of dynamic pressure at P'(3), (b) Mode analysis to longitudinal direction.....	38
Fig 3.11	Mode analysis about instability of 500 Hz (a) FFT result of dynamic pressure at P'(3), (b) Mode analysis to longitudinal direction.....	38
Fig 3.12	Image postprocessing for enhancing contrast	40
Fig 3.13	FFT results of the length of the unburned region in stable and unstable flames	42
Fig 3.14	Change tendency of the unburned region and phase relation between p' , q' and the length of the unburned region of 2 nd mode case	43
Fig 3.15	Change tendency of the unburned region and phase relation between p' , q' and the length of the unburned region of 3 rd mode case	44
Fig 3.16	Instability frequencies of fully premixed flame and	

partially premixed flame varying equivalence
ratio.....46

Fig 3.17 Averaged OH chemiluminescence images of
partially and fully premixed flames at two different
equivalence ratio conditions (0.7, 0.82)48

Chapter 1 INTRODUCTION

1.1 Combustion instability

As environmental problems arise from global warming, interests in emission gases like NO_x and CO, which is main cause of global warming, is increasing and many researches about emission gases have been performed. In a gas turbine industry, the most commonly used method is a lean premixed combustion. The lean premixed combustion, which has a low flame temperature compared to stoichiometric condition due to excess oxidant, have an advantage that the emission gases like NO_x and CO can be remarkably reduced. However, the lean premixed combustion is susceptible to combustion stability because it have high probability of combustion instability.

Combustion instabilities occur in the form of large-amplitude oscillations of natural acoustic modes of the combustor. The large-amplitude oscillations in the combustor have adverse effects on lifetime of mechanical components, which is presented in fig 1.1, thrust oscillation and flame blowoff or flashback and these adverse effects

may result in reliability of gas turbine engine. Generally, the combustion instabilities are occurred due to positive feedback loop between flow/mixture perturbations, heat release oscillations and acoustic oscillations. This feedback loop is shown in fig 1.2.

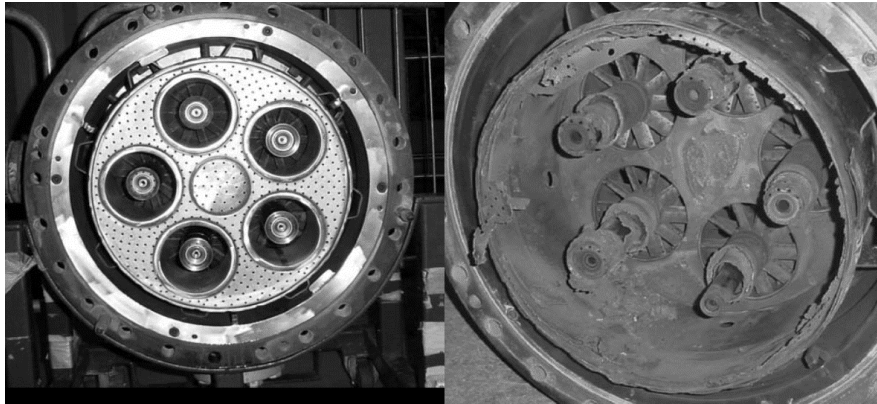


Figure 1.1 Two burner assemblies, left : intact , right : damaged due to instability

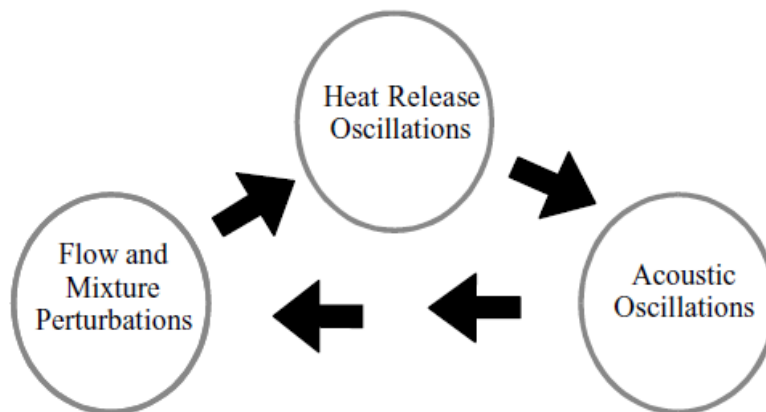
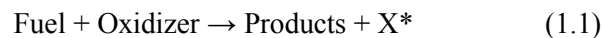


Figure 1.2 Feedback loop of the combustion instability [1]

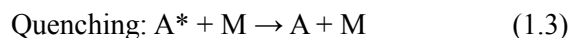
Therefore, many studies about characteristics of the combustion instability in gas turbine combustor have been carried out recent years.

1.2 OH chemiluminescence

Chemiluminescence is the emission of light from spontaneous emission, as the result of a chemical reaction. When molecules with an excited state due to result of chemical reaction falls to a low energy level, light, which is called as chemiluminescence, is emitted. The reaction between fuel and oxidizer is shown in Eq 1.1.



The X^* presented in Eq 1.1 means an excited molecule, which is produced during chemical reaction process. And the excited molecule may be destroyed by spontaneous emission or quenching process. Process of spontaneous emission and quenching process are presented in Eq 1.2 and Eq 1.3 respectively.



Light from spontaneous emission corresponds to chemiluminescence. During spontaneous emission, the photons, which have energy, equal to difference of

energy level before and after the reaction, are emitted. And its wavelength is calculated from energy difference divided by Planck' constant.

During combustion processes of hydrocarbon fuels like methane, propane, octane etc. chemiluminescence light from OH, CH, C₂, CO₂ radicals are emitted and its corresponding wavelengths and spectrum are presented in table 1.1 and fig 1.3 [2] . Excited OH radicals, which is mainly located high temperature burned gases, and excited CH radicals, which mainly exists in narrow reaction zone of flames are most commonly used radicals visualizing flame structure. Therefore, flame structures can be photographed using camera with appropriate bandpass filters, which transmit only light of desired wavelength from flames.

Radical	Transition	λ (nm)
OH*	$A^2\Sigma^+ \rightarrow X^2\Pi$ ($\Delta v=1$)	282.9
OH*	$A^2\Sigma^+ \rightarrow X^2\Pi$ ($\Delta v=0$)	308.9
CH*	$B^2\Sigma^- \rightarrow X^2\Pi$	387.1
CH*	$A^2\Delta \rightarrow X^2\Pi$	431.4
C_2^*	$A^3\Pi_g \rightarrow X^3\Pi_u$ (Swan)	516.5
CO_2^*	Continuum	350 ~ 500

Table 1.1 Typical radicals from hydrocarbon fuel combustion process

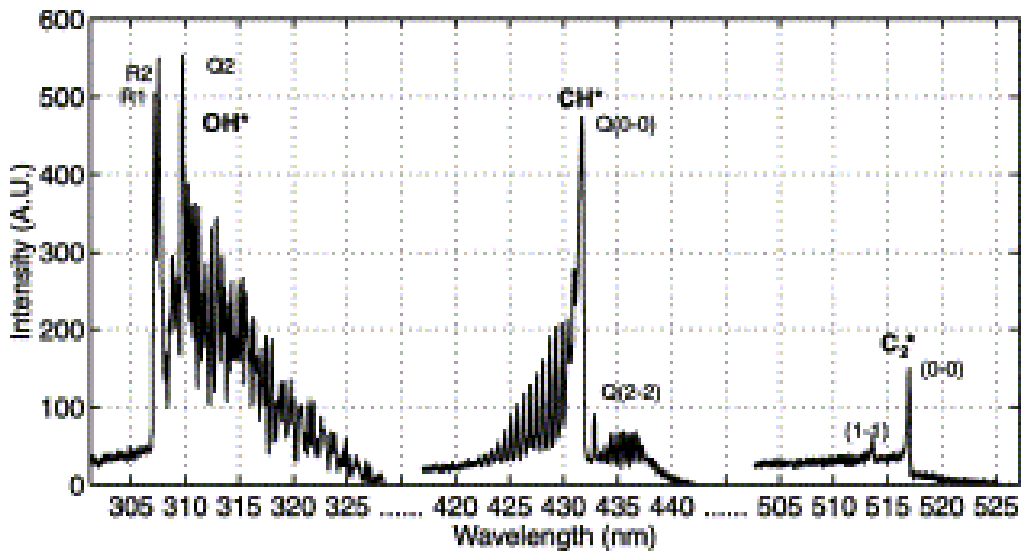


Figure 1.3 Spectrum of chemiluminescence light from typical flames [2]

1.3 OH planar laser induced fluorescence (OH-PLIF)

Before introducing OH planar laser induced fluorescence (OH-PLIF) method, laser induced fluorescence should be explained. Laser induced fluorescence, which was called as LIF, is a spectroscopic method in which molecules are excited to a higher energy level by the absorption of laser light corresponded to spontaneous emission of light. When molecules are exposed to light, which have the wavelength of spontaneous emission light, molecules absorb the light and are raised up to higher energy level. Then these molecules fall down to lower energy level emitting light, which have distinct wavelength from incident laser light.

Planar laser induced fluorescence (PLIF) means LIF technique extended to two dimensions using laser sheet from pulsed laser.

OH-PLIF method have been typically used to obtain spatially and temporally resolved images of the reaction zone of various flames. The OH radical concentration increases rapidly around the flame region in about 20 μ s and then destroys slowly in 1 to 5 ms by a 3-body recombination reaction as described in table 1.2. Therefore,

super equilibrium OH radicals exists at the flame front and these OH radicals have a concentration more than about ten times that that of O or H radicals. Thus, fluorescence signal from the OH radical is more intense than that of other radicals. Because of this reason, the fluorescence signal of the OH radical is widely used as an indicator of flame front in reacting flow.

Fast OH formation by two-body reactions (1~5 ms)
$\text{H} + \text{O}_2 \leftrightarrow \text{OH} + \text{O}$ $\text{O} + \text{H}_2 \leftrightarrow \text{OH} + \text{H}$ $\text{H} + \text{HO}_2 \leftrightarrow \text{OH} + \text{OH}$
Slow destruction by three-body recombination reactions (~20μs)
$\text{H} + \text{OH} + \text{M} \leftrightarrow \text{H}_2\text{O} + \text{M}$

Table 1.2 Formation and destruction processes of OH radical

In OH-PLIF method, the Q₁(8) line of the A-X(1,0) band of the OH radical is used for excitation of OH radicals. The fluorescence signal from the A-X (1,0) and (0,0) bands which have wavelength of about 310nm.

1.4 Particle image velocimetry (PIV)

Particle Image Velocimetry (PIV) is an optical method of flow visualization for obtaining velocity vector fields by comparing consecutive two images. It is a method to calculate the direction of flow through two consecutive images taken at certain intervals. Particle seeding procedure is a prerequisite of PIV method. Mie scattering signal from seeding particles are used for capturing flow images. Many kinds of particles have been used for fluid tracer, and Al_2O_3 typically is used for non-reacting flow and ZrO_2 are commonly used for high temperature of reacting flow due to high melting temperature.

Generally, a double pulsed Nd-YAG laser is used as a light source and a high speed CCD camera or CMOS camera are employed to obtain instantaneous particle images taken mie scattering signal of seeding particles at a measurement plane. There are no specific rules for particle seeding system; however, the size of particle should be determined by considering whether particles can follow the flow well or not.

Using consecutive images through certain processes, the displacement of the particles are calculated. The principle of the typical PIV system is presented in fig

1.4. It is necessary to divide the image into grids to calculate velocity vector fields. The grids are called as an interrogation spots. After setting the interrogation spot size, one interrogation spot of the first images is picked and compared with all the interrogation spot of the second images. The displacement between the interrogation spot of the first image and the interrogation spot of the second image represents one vector of flow field. By conducting this work in all the interrogation spots, whole vectors of flow-field are obtained. This process is called as a cross correlation.

As a result, PIV is a method of calculating velocity vector fields through the cross correlation method using consecutive images of particles, which is well followed real flow, taken continuously at certain time intervals.

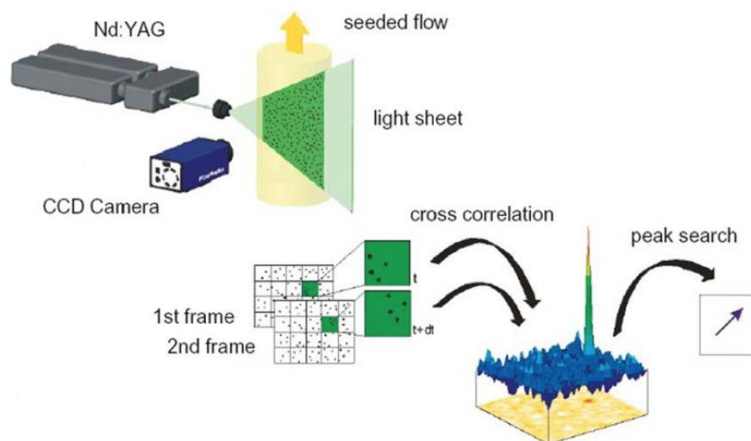


Figure 1.4 Principle of typical PIV system

1.5 Overview of present works

Recently, many researches about combustion instability characteristics and its mechanisms in gas turbine combustor have been actively reported.

Several research groups conducted researches about occurrence mechanisms of combustion instabilities. T. Lieuwen et al. conducted study about the mechanism of transfer of pressure fluctuation to the heat release oscillations in premixed flames. Due to explain these mechanisms, characteristic delay times in each steps based on the Rayleigh's criterion were introduced to explicate occurrence of combustion instabilities [3]. Ducruix et al. investigated the effects of various factors like flame/boundary interaction, flame/vortex interaction, and strain rate on flame and how they affect acoustic and heat release waves [4].

Studies about characteristics of combustion instabilities were carried out. R. Balachandran et al. conducted study about mode shifting phenomenon in bluff body combustor. They confirmed that the instability frequency leap up to higher frequency as equivalence ratio increases [5]. Yoon et al. also conducted study about mode shifting phenomenon in partially premixed model gas turbine using mixture of

methane and hydrogen as a fuel. It is confirmed that the frequency of combustion instability increased as the ratio of the hydrogen in fuel increases. The concept of convective delay time, which calculated using distance from nozzle to flame and exit velocity of fuel-air mixture at nozzle, were introduced to explain mode shifting phenomenon [6]. Lee et al. investigated several time delays between pressure fluctuation and oscillations of heat release rate in model gas turbine combustor which used syngas as a fuel. It was confirmed that the convective delay time occupy the largest proportion of total time delay between pressure fluctuation and oscillation of heat release rate [7].

Study about flame structure in unstable flames also was also conducted. S. Taamallah et al. investigated research about flame structural characteristics in unstable flames. Structure of flames was categorized into five category according to equivalence ratio increase in premixed combustor. And structural difference between stable and unstable flame also investigated [8].

The response of the flame to mixing degree of fuel and air was also studied. A. M. Kypraiou et al. conducted about response of flames with different premixedness. The three premixing types; fully premixed, non-premixed with radial fuel injection and

non-premixed with axial fuel injection were investigated. It was confirmed that responses to acoustic oscillations are different in three premixing types and type of non-premixed with radial fuel injection has the highest response to acoustic oscillations.

Therefore, in this study, effects of flow rate change on combustion instability were investigated in partially premixed combustor. Effects of large scale variation and effects of small scale variation were verified. When large scale of flow rate change occurs in flame, the frequency of combustion instability varied as flow rate changes. So, concept of convective delay time was introduced to analyze relationship between instability frequency and flow rate changes.

And second part of this study, effects of small scale variation were investigated. When combustion instability occurs, small scale variation of flow rate at nozzle is produced due to pressure fluctuation in combustor. Effects of small scale variation on instability frequency and flame structure were confirmed comparing fully premixed flame and partially premixed flame.

Chapter 2 APPARATUS AND EXPERIMENTAL METHOD

2.1 Model gas turbine combustor

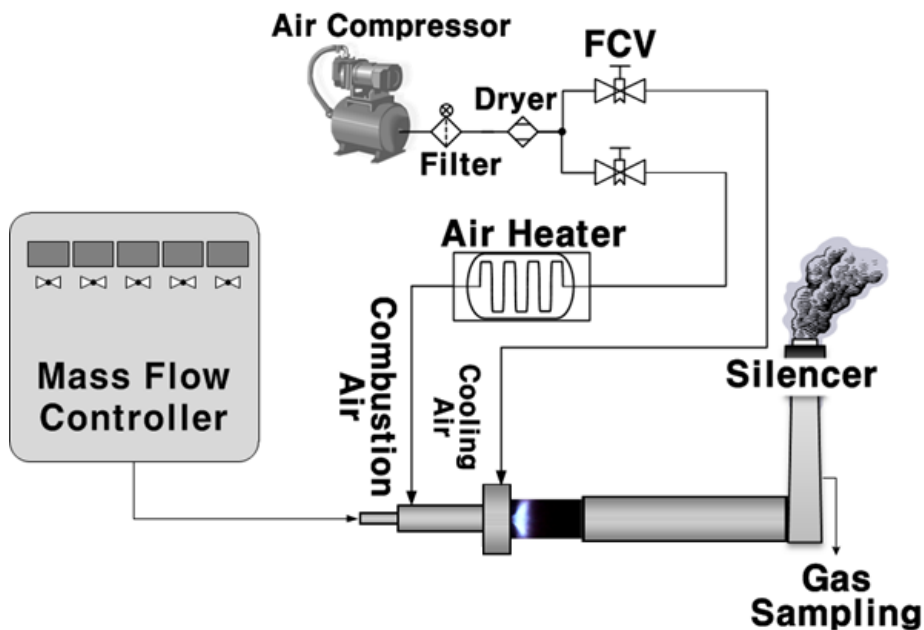


Figure 2.1 Schematic of test facility

The schematic of test facility is shown in Figure 2.1. It consists of an air heater, several mass flow rate controller for fuel and air, a combustor section and an exhaust duct. The preheated air using the air heater and fuel, which have 300K of temperature, are used. And the end of the facility, there is gas analyzer for detecting exhaust gases, like CO, NO etc. Air and fuel are injected through partially

premixed type swirler, which have 14 guide vanes inclined at 45° and each have a 1.78 mm diameter fuel injection hole, and its swirler number is about 0.8. Detailed shape of the swirler can be seen in figure 2.2.

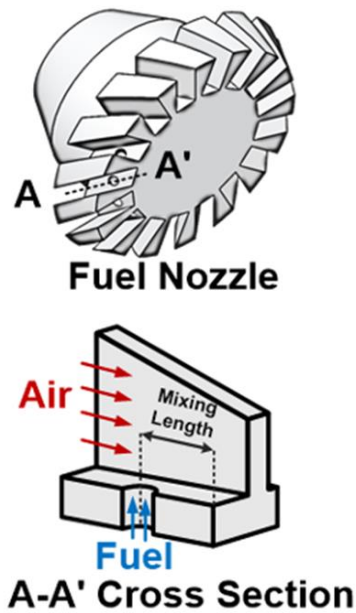


Figure 2.2 Schematic of partially premixed type swirler

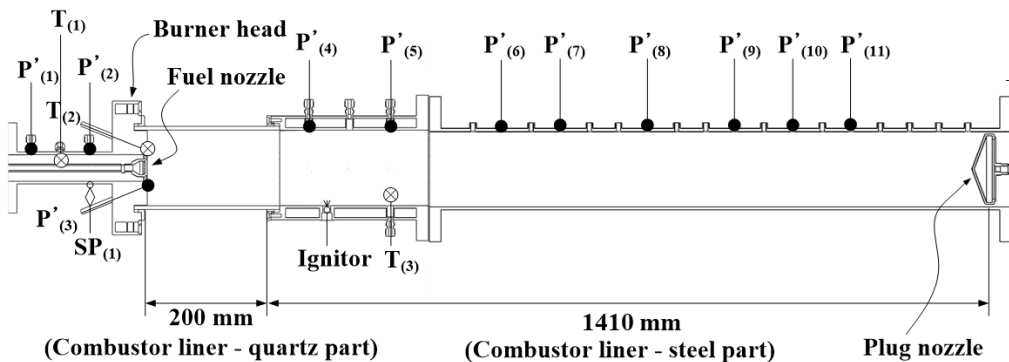


Figure 2.3 Schematic of model gas turbine combustor

Schematic of model gas turbine combustor used in this study is presented in figure 2.3. It has eleven dynamic pressure sensors (PCB 102A05) and three thermocouples along the combustor for detecting longitudinal mode of combustion instability and its locations are also shown in figure 2.3. The dynamic pressure measured at the port 3, which was expressed as $P'(3)$ at the dump plane in fig 2.3, was used to determine whether combustion instability occurs or not. A 200mm long quartz tube, which is being cooled by cooling air from a compressor, is mounted behind the swirler for flame visualization. And a water-cooled plug nozzle, which has about 90% of blockage ratio of the combustor area to form acoustically closed boundary condition, is installed in the end of the combustor and it can be able to move back and forth.

2.2 Diagnostics setup

In this study, OH chemiluminescence imaging, OH-PLIF and PIV measurement were carried out to visualize flame structure and flow field in combustor. All measurements were synchronized with signal of dynamic pressure.

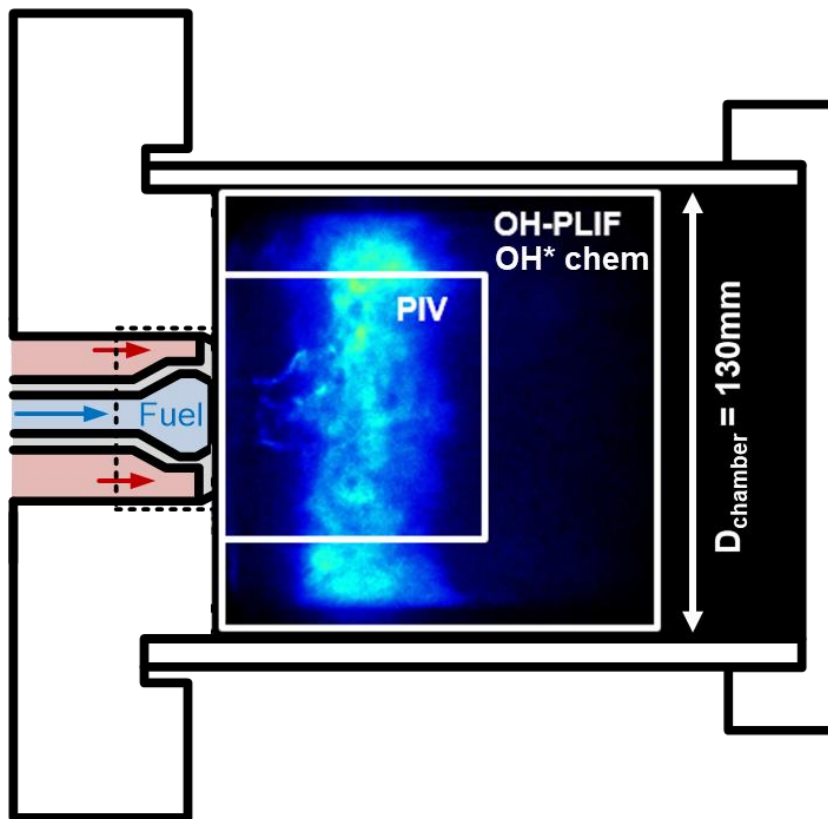


Figure 2.4 Region of interest of each measurement techniques.

Regions of measurement techniques are shown in fig2.4. For a full range of the quartz with a diameter of 130mm, OH chemiluminescence and OH-PLIF measurements were employed and for PIV measurement, the region of 65mm × 65mm was measured. Detail setup for each measurements are as follow.

2.2.1 Setup for OH chemiluminescence

High speed CMOS camera (High-speed star8, Lavision), which is shown in fig 2.5 was employed to detect fluorescence signal of OH radicals formed during combustion process, which is good indicator of the reaction zone of the premixed flame to observe overall flame structure and heat release rate. Chemiluminescence images were taken during 1 s at 7 kHz repetition and it had 1024 × 1024 pixels of spatial resolution and appropriate bandpass filter, which have range for wavelength of 310 nm, was also installed.



Figure 2.5 High speed CMOS camera, intensifier and programmable timing unit.

2.2.2 Setup for OH-PLIF

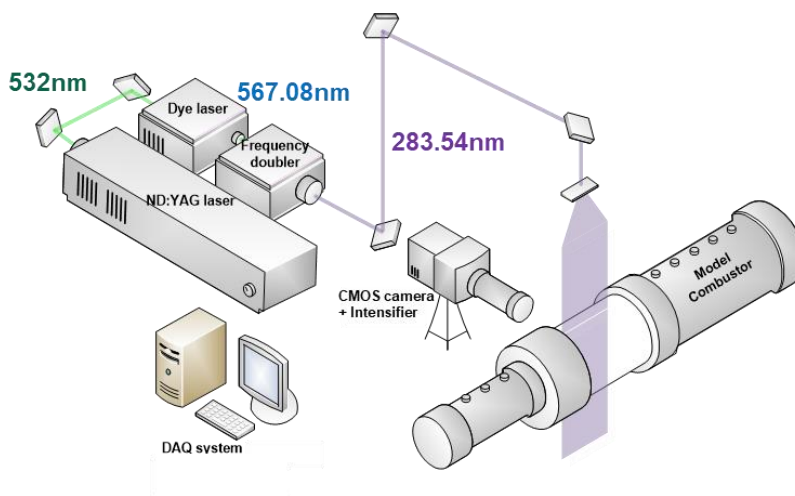


Figure 2.6 Optical setup for OH-PLIF measurement

Optical setup for OH-PLIF measurement are presented in fig 2.6. Laser in the 532nm wavelength range, which was emitted from ND:YAG laser (IS 200-2L, Edgewave) is used for source laser and it passes through a Dye laser(Credo Dye, Sirah) using Rhodamine 6G as dye solution and a frequency doubler, and turns into laser in the 283.54 wavelength. Same high speed CMOS camera used for OH chemiluminescence imaging was used for OH-PLIF measurement. Images were taken during 1 s using an appropriate bandpass filter at same spatial and temporal resolution as setting of the OH chemiluminescence imaging.

2.2.3 Setup for PIV

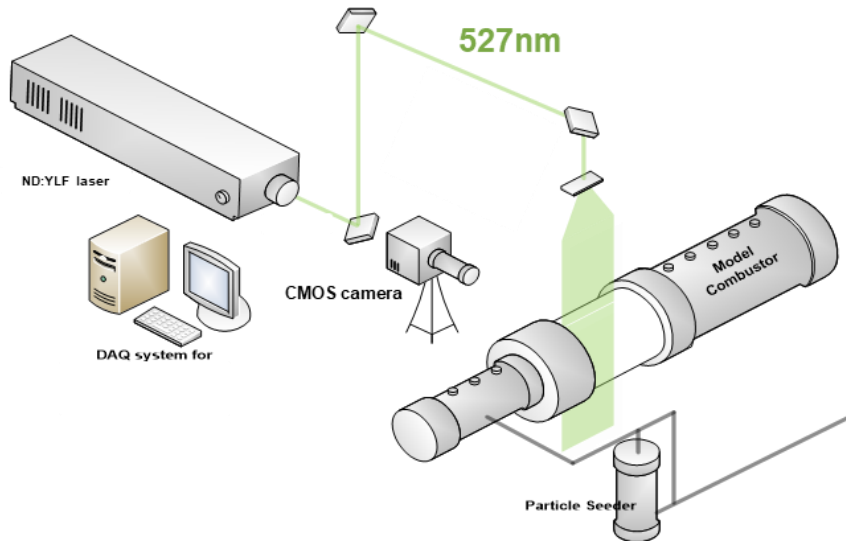


Figure 2.7 Optical setup for PIV measurement

For calculation of velocity field in combustor, PIV measurement were employed and its optical setup is shown in fig 2.7. ND:YLF laser which have wavelength of 527nm was used for incident laser and signal of mie scattering from seeding particle was captured using high-speed CMOS camera (High-speed star8, Lavisision). Zirconium oxide of 1.5 μm diameter was used. It is suitable for measurement of combustion phenomena, which occurs in high temperature, because it have a high melting point. It was seeded into air flow through particle

seeder. Images of a $65\text{mm} \times 65\text{mm}$ region were taken with 1024×1024 pixel and 3.5 kHz repetition rate. Appropriate bandpass filter, which have high transmittance at the wavelength of mie scattering signal, was installed in front of the camera. Two laser pulses were incident at an interval of $6 \mu\text{s}$. The velocity fields were calculated by using the multi-path cross correlation algorithm and size of the interrogation window was set to 32×32 pixels and 16×16 pixels.

2.2 Test condition

In this study, Effects of the change of the fuel and air flow rate in combustion instability in partially premixed combustor were investigated.

First, when a large change in flow rate occurs, the phenomena that frequency of combustion instability changed according to equivalence ratio change under constant air flow rate was found. Therefore, experiments were carried out with varying fuel and air flow rates, i.e., at various equivalence ratio and mean velocity conditions to analyze the effect of the large scale variation of flow rate on the instability frequency. The equivalence ratio was increased by increasing fuel flow rate under constant air flow rate or decreasing air flow rate at constant fuel flow rate. And, to confirm effect of change of total flow rate, change of the instability frequency was measured by increasing total flow rate based on the air flow rate.

Detailed experimental conditions are presented in table 2.1. Pure methane gas was used for fuel and air, which was preheated to 200°C for mimicking a high temperature and high pressure combustion environment of a real gas turbine combustor at 1 atm, was used for oxidizer. The length of the combustor was set to 1410 mm. When changing the equivalence ratio from 0.6 to 0.9, the fuel and air flow rate was fixed

to 69 slpm and 1100 slpm respectively and the other flow rate was changed to raise the equivalence ratio. And when confirming the effect of the total flow rate, the air flow rate was changed from 688 slpm to 1375 slpm.

Parameters	Values
Fuel	CH ₄
Combustor Length [mm]	1410
Air Inlet Temperature [K]	473
Equivalence ratio	0.6 ~ 0.9 (span = 0.02) (Air fixed 1100slpm ,Fuel fixed 69slpm)
Air flow rate [slpm]	688 ~ 1375 (span = 137.5)

Table 2.1 Experimental conditions

Second, effects of small scale change of flow rate on flame structure and instability frequency were also investigated. The structure of flame was analyzed for only two cases with instability frequency of 500 Hz and 750 Hz, which have air flow rate of

1100 slpm, because 500 Hz and 750 Hz of combustion instability occurred under most experimental conditions.

Chapter 3 RESULTS AND DISCUSSION

3.1 The effect of the large-scale variation

In this chapter, the flame position and the exit velocity of the fuel-air mixture at nozzle were investigated for explaining the relationship between the variation of the instability frequency and the change of the convective delay time. As mentioned before in the previous chapter, the experiments were divided into three categories. The first category is equivalence ratio increase raising the fuel flow rate under constant air flow rate. The second one is equivalence ratio increase reducing the air flow rate. The last one is increasing total flow rate under same equivalence ratio.

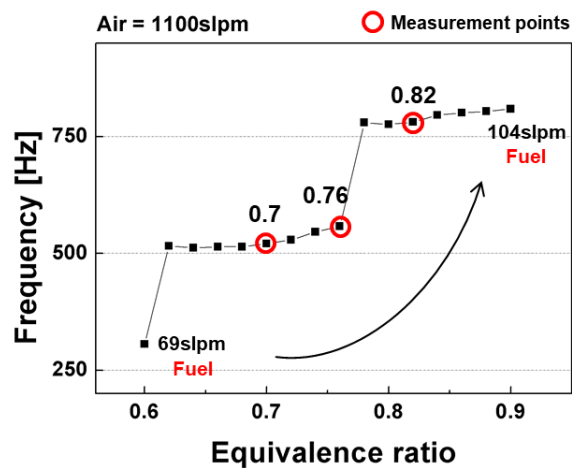


Figure 3.1 Instability frequency change increasing fuel flow rate (air = 1100 slpm)

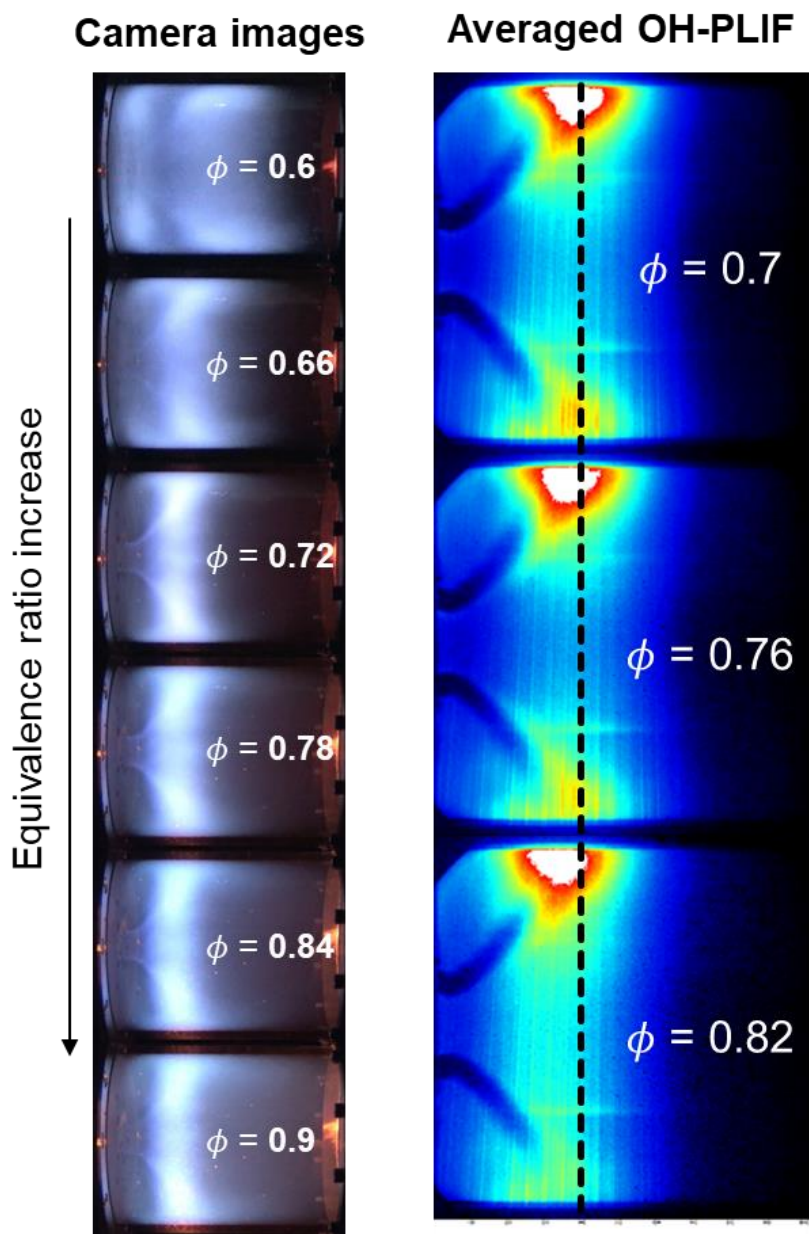


Figure 3.2 Direct flame images and averaged OH-PLIF images increasing fuel flow rate (air = 1100 slpm)

First, the instability frequency, the flame position and the exit velocity of the mixture were observed while the equivalence ratio was raising by increasing the fuel flow rate. When the equivalence ratio increases, the instability frequency increases from about 250Hz to about 750Hz as presented in fig 3.1. Direct flame images were taken to determine the variation of the flame position using camera and OH-PLIF and PIV measurements were adapted for visualizing cross-sectional images of the flame and the velocity fields in the combustor. The three red circles in fig 3.1 mean the target conditions of the laser diagnostics like OH-PLIF and PIV.

The direct images taken using camera and the averaged OH-PLIF images were presented in fig 3.2. As can be seen in the direct flame images of the fig 3.2, the flame position gradually moves toward the dump plane as the equivalence ratio increases and the same tendency can be confirmed in the averaged OH-PLIF images of the fig 3.2. Also, it can be found that in the most fuel rich condition, the flame is nearest to the dump plane.

And the tendency of the exit velocity of the fuel-air mixture was also investigated for calculating the convective delay time. The variation of the exit velocity is presented in figure 3.3.

In this case, since the fuel flow have relatively small flow rate compared to the air flow, there is no significant change of the flow rate of the fuel-air mixture.

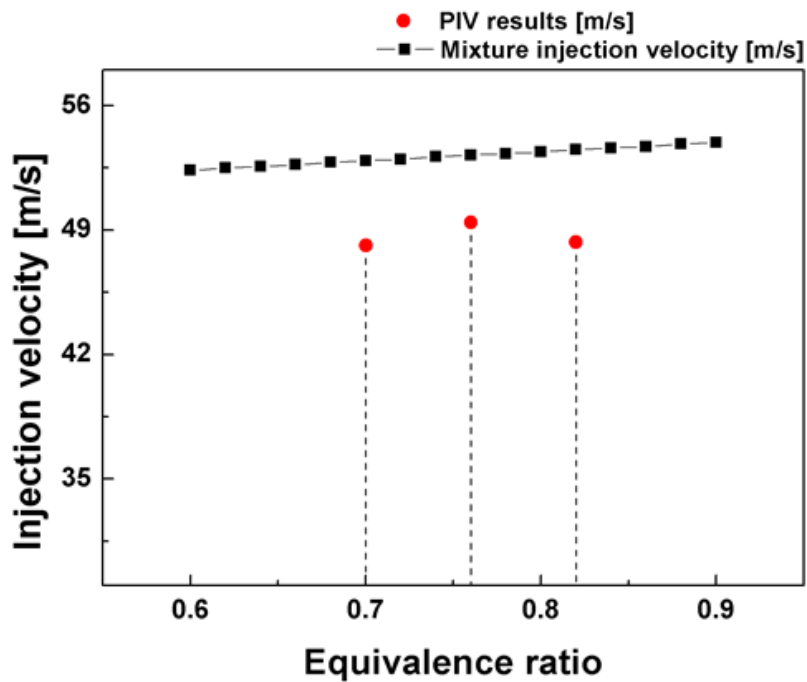


Figure 3.3 Injection velocity change increasing fuel flow rate (air = 1100 slpm)

Therefore, the exit velocity of the fuel-air mixture does not change much as equivalence ratio increases. PIV measurements were conducted for three equivalence ratio conditions shown in fig 3.1 as red circle to see whether the same tendency that the exit velocity does not change much as equivalence ratio increases can be confirmed in actual flow field in the combustor. The results of the PIV

measurements are marked as red dot in the fig 3.3. Since the velocities, which have three-dimensional direction were measured by using PIV measurement, which used to measure the velocity of the two-dimensional direction, it can be seen in the fig 3.3 that although the error is present, the exit velocity of the fuel-air mixture does not change much in spite of the increase of the equivalence ratio.

So in this case, as the equivalence ratio increases, the flame position gradually moved toward the dump plane, but the exit velocity of the fuel-air mixture is almost same. Therefore, as a result of the shortened convective delay time due to the change of the flame position and exit velocity of the fuel-air mixture, the frequency of the combustion instability increases as the equivalence ratio increases.

Second, the instability frequency, the flame position and the exit velocity of the mixture were investigated while the equivalence ratio was raising by decreasing the air flow rate.

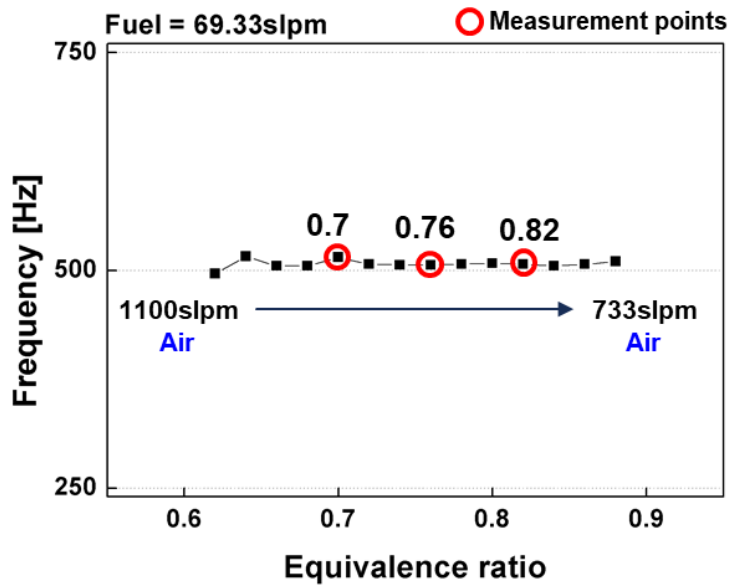


Figure 3.4 Instability frequency change decreasing air flow rate (fuel = 69 slpm)

The change of the instability frequency according to the change of the equivalence ratio can be seen in fig 3.4. Unlike the previous case, in this case, the frequency of the combustion instability kept almost constant even when the equivalence ratio was increased. To find reason why the instability frequency does no change much even when the equivalence ratio was increased, the flame position and the exit velocity at the nozzle were investigated like previous case.

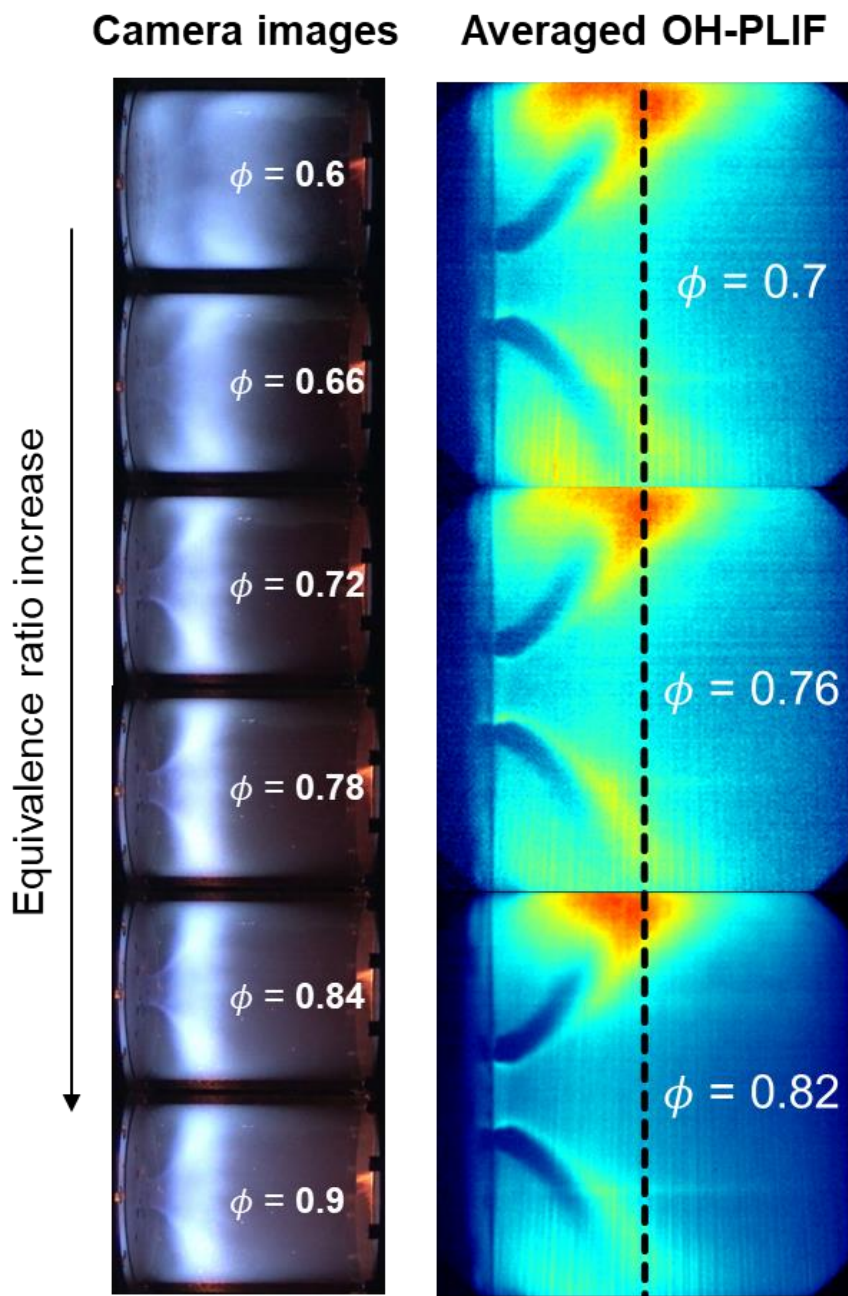


Figure 3.5 Direct flame images and averaged OH-PLIF images decreasing air flow rate (fuel = 69 slpm)

The change of the flame position decreasing the air flow rate is shown in fig 3.5. As results of the previous case, it can be found that the flame moved toward to the dump plane as the equivalence ratio increases in both direct flame images and the averaged OH-PLIF images.

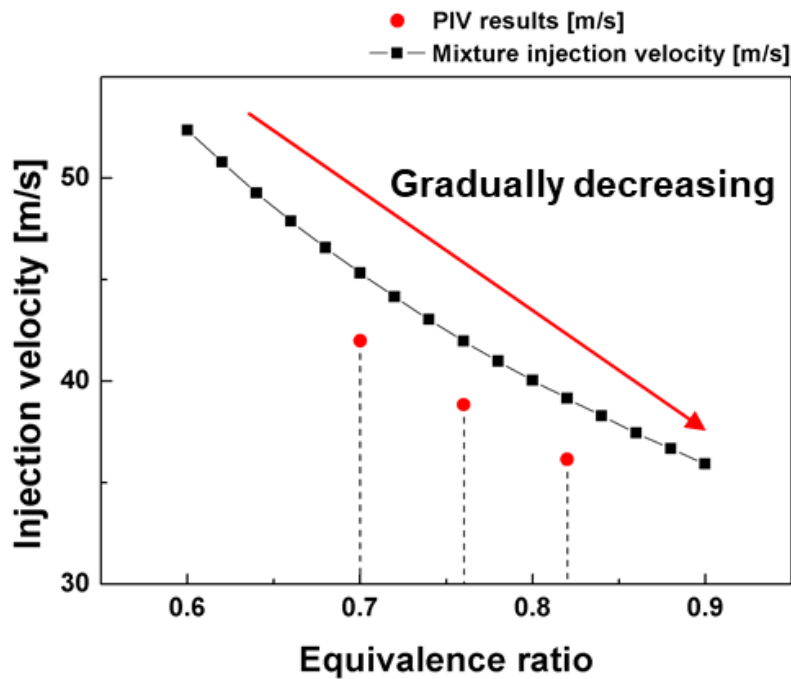


Figure 3.6 Injection velocity change decreasing air flow rate (fuel = 69 slpm)

The exit velocity of the fuel-air mixture also measured in this case. The tendency of the exit velocity is presented in fig 3.6. Unlike the previous case, the flow rate of the mixture decreases as the equivalence ratio increases because the air flow occupies a large proportion in the total mixture flow. So, the exit velocity of the fuel-

air mixture fall down gradually as the equivalence ratio increases.

Therefore, when the equivalence ratio was increased by decreasing the air flow rate, the flame moved toward the dump plane and the exit velocity of the fuel-air mixture at the same time as the equivalence ratio increases. The change of the flame position and the decreasing exit velocity influence contradictory effect on the convective delay time, so the convective delay time keeps almost constant and the frequency of the combustion instability also remains almost same.

Last, the effects of the total flow rate on the flame position and the exit velocity were elucidated. The experiments were performed increasing overall flow rate by increasing the air flow rate under several fixed equivalence ratio.

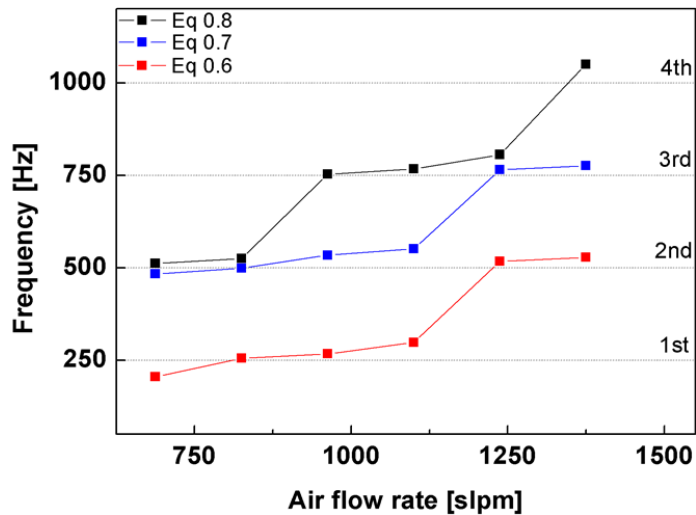


Figure 3.7 Instability frequency change increasing air flow rate under constant equivalence ratio

The trend of the instability frequency under several equivalence ratio (0.6, 0.7, 0.8) is presented in fig 3.7. As shown in fig 3.7, the instability frequency increases as the air flow rate increases in all of the three equivalence ratio conditions. Likewise, the flame position and the exit velocity at the nozzle were investigated to explain why the instability frequency increases.

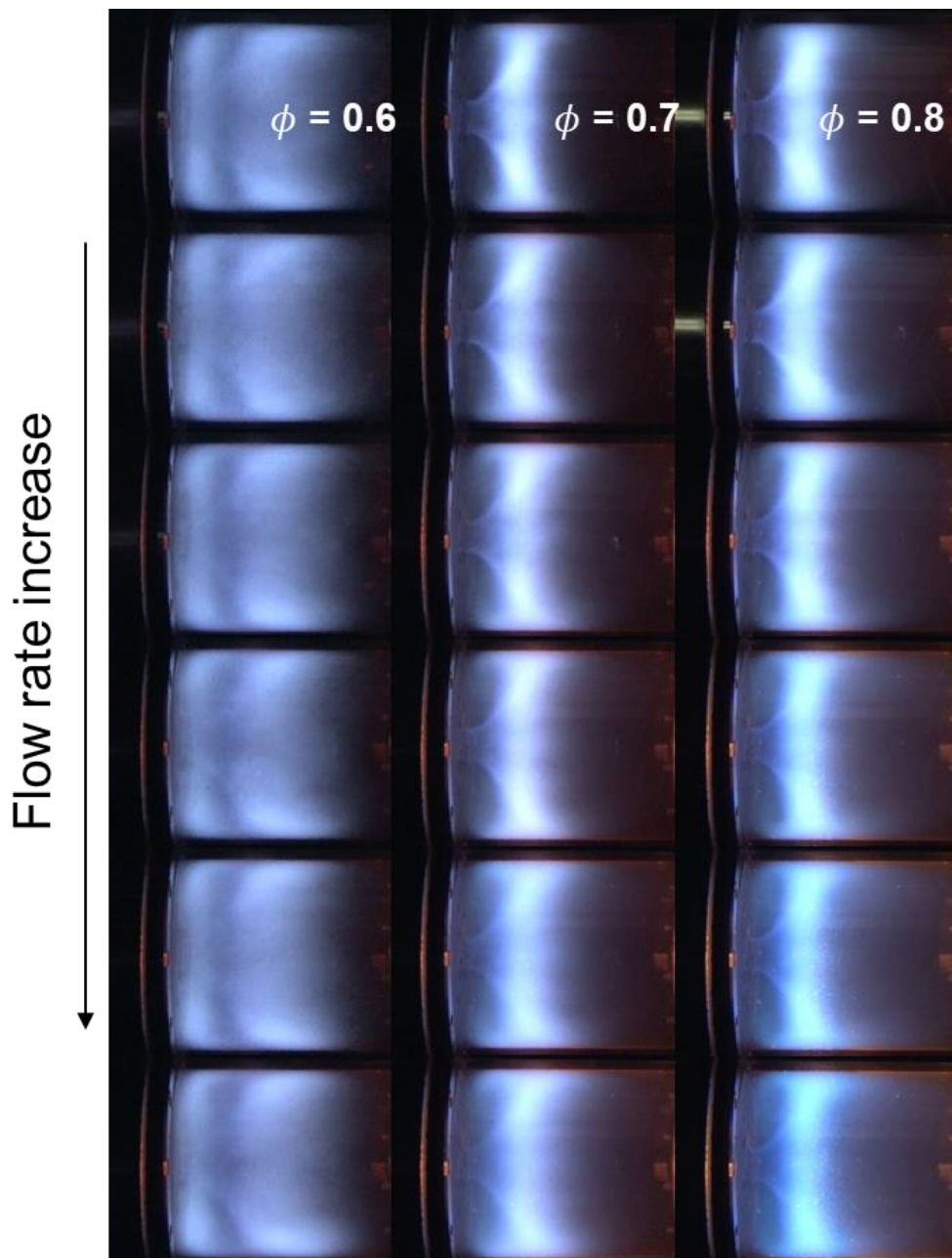


Figure 3.8 Direct flame images increasing flow rate under constant equivalence

ratio

Despite the increasing overall flow rate, the position of the flame kept almost same except for minor changes due to change of the mean velocity of the mixture as shown in fig 3.8.

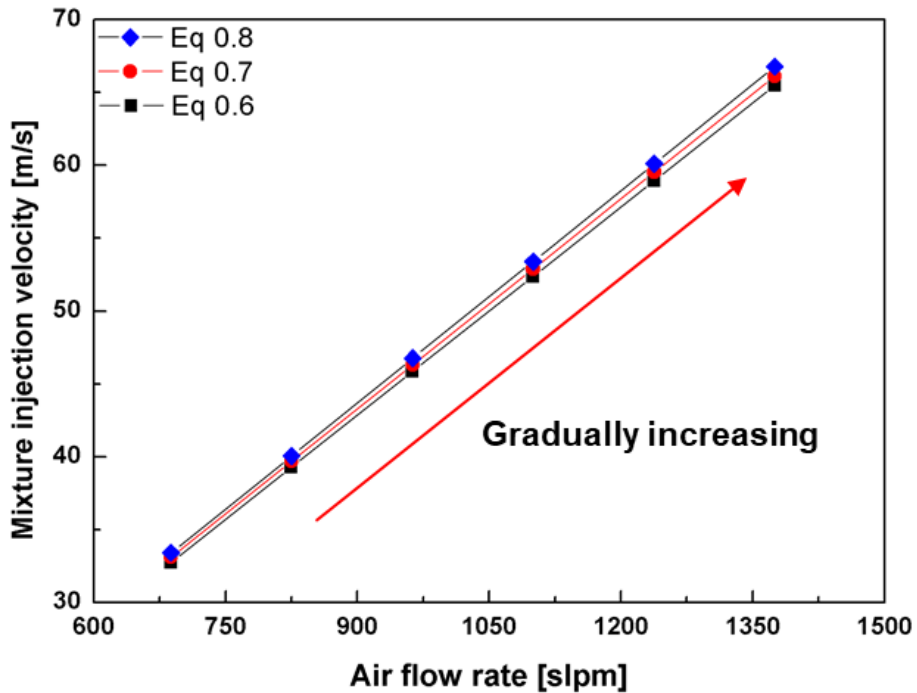


Figure 3.9 Injection velocity change increasing air flow rate under constant equivalence ratio

The variation of the injection velocity at the nozzle with increasing air flow rate is shown in fig 3.9. As the air flow rate increases, the total flow rate increases as a matter of course, so the injection velocity at the nozzle also increases.

Therefore, as the air flow rate increases, the position of the flame had not changed significantly, but the convective delay time is shortened due to increase of the injection velocity. And the shortened convective delay time influenced the increase of the frequency of the combustion instability.

2.2 The effect of the small-scale variation

When the combustion instability occurs, pressure fluctuation also occurs in the combustor, which influence injection velocity at the nozzle, so small-scale flow rate change appears. The effects of small-scale flow rate change on the flame structure and instability frequency were investigated in this chapter. It is difficult to analyze all of the experimental cases, so two representative cases, which have about 500 Hz and 750 Hz of instability frequency under 1100 slpm of air flow rate were chosen because almost conditions have 500 Hz and 750 Hz of instability frequency. Mode analyses were conducted to find out mode of instability frequencies of 500 Hz and 750 Hz using signals of seven dynamic pressure sensors in the longitudinal direction from dump plan to plug nozzle which is located at the end of the combustor. Results of mode analyses are summarized in fig 3.10 and fig 3.11. As results, the instability frequencies of 500 Hz and 750 Hz corresponds to 2nd and 3rd longitudinal mode respectively. Therefore, each case was referred as 2nd mode case and 3rd mode case.

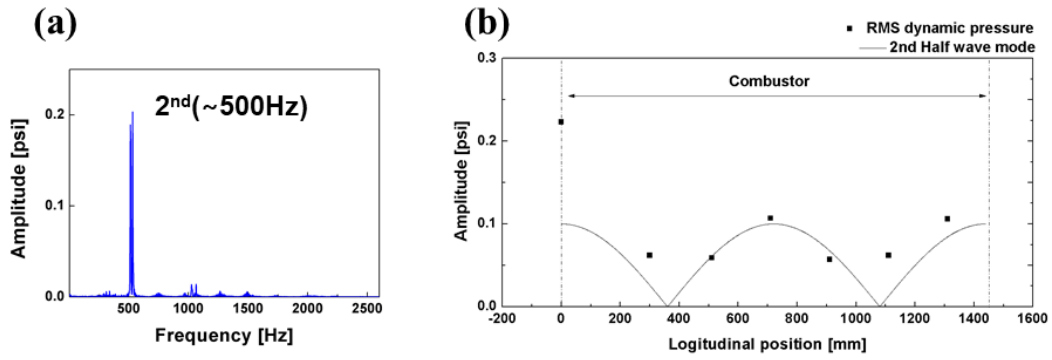


Figure 3.10 Mode analysis about instability of 500 Hz

(a) FFT result of dynamic pressure at P'(3), (b) Mode analysis to longitudinal direction

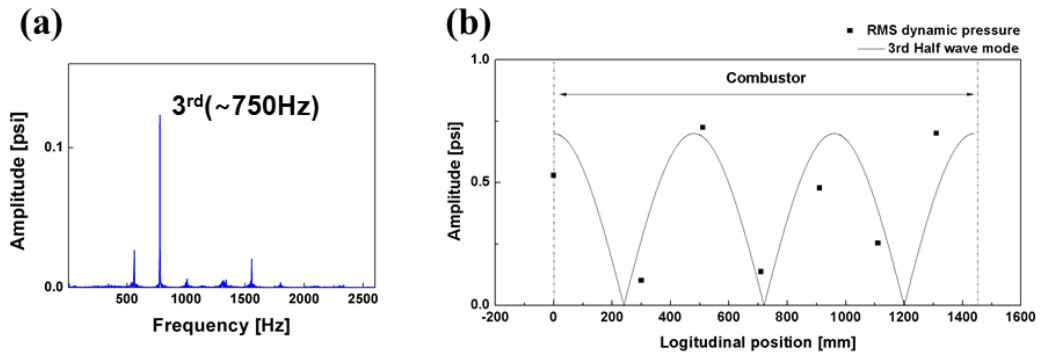


Figure 3.11 Mode analysis about instability of 750 Hz

(a) FFT result of dynamic pressure at P'(3), (b) Mode analysis to longitudinal direction

Before analyzing flame structure, stable flame conditions were sought in spite of same flow condition for comparing flame structure of unstable flames to structure of stable flames. In general, combustion instability occurs due to positive coupling mechanisms between fluctuation of heat release rate and acoustic oscillation. For making stable flames, fluctuation of heat release rate and acoustic oscillation were artificially decoupled by modification of combustor length from 1410 mm to 1210 mm. Therefore, comparisons between stable flames and unstable flames in order to find out the inherent flame structural characteristics of unstable flames.

The change of unburned region in instantaneous OH-PLIF images was intensively observed to confirm the influence of small-scale flow rate changes on the flame structure. Generally, the unburned region is formed due to the presence of the region before the reaction zone, which is necessary for fuel-air mixture required to be heated to the ignition temperature, in premixed flame. However, in the case of the partially premixed flame used in this study, the region where injected fuel and air are mixed for combustion also affects the formation of the unburned region in addition to the preheating zone of the premixed flame.

The process in which the pressure fluctuation in combustor leads to changes in length of the unburned region is as follows. At first, the pressure perturbation at the

flame is transmitted to nozzle and transmitted pressure perturbation makes change of fuel and air flow rate. At that time, the change of flow rate and injection velocity of fuel and air flow are different because the pressure drop of fuel and air flow at the nozzle does not same. As a result, when pressure perturbation is transmitted to nozzle, degree of fuel-air mixing is changed by changed jet momentum ratio. And length of the unburned region also is also varied due to changed time, that is the time required for complete mixing of fuel-air mixture.

FFT analysis was performed to see if the length of the unburned region changes in unstable flames. Prior to FFT analysis, some image processing techniques were employed to enhancing contrast of instantaneous OH-PLIF images.

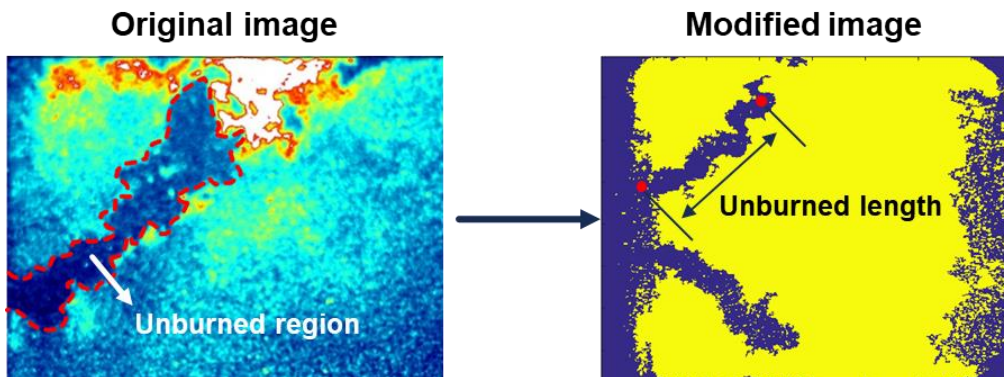


Figure 3.12 Image postprocessing for enhancing contrast

Original instantaneous OH-PLIF image and modified image for calculation the length of the unburned region are shown in fig 3.12. The methods of binarization and histogram equalization were carried out to distinguish the unburned region. And then, distance from exit of the nozzle to end of the unburned region was calculated.

Through the above image processing process, the variation frequencies of the length of the unburned region were calculated. The results are presented in fig 3.13. In unstable flames, unlike stable flames, it was confirmed that the change of the length of the unburned region has a specific frequency, which respectively corresponds to frequency of the combustion instability in 2nd mode and 3rd mode cases.

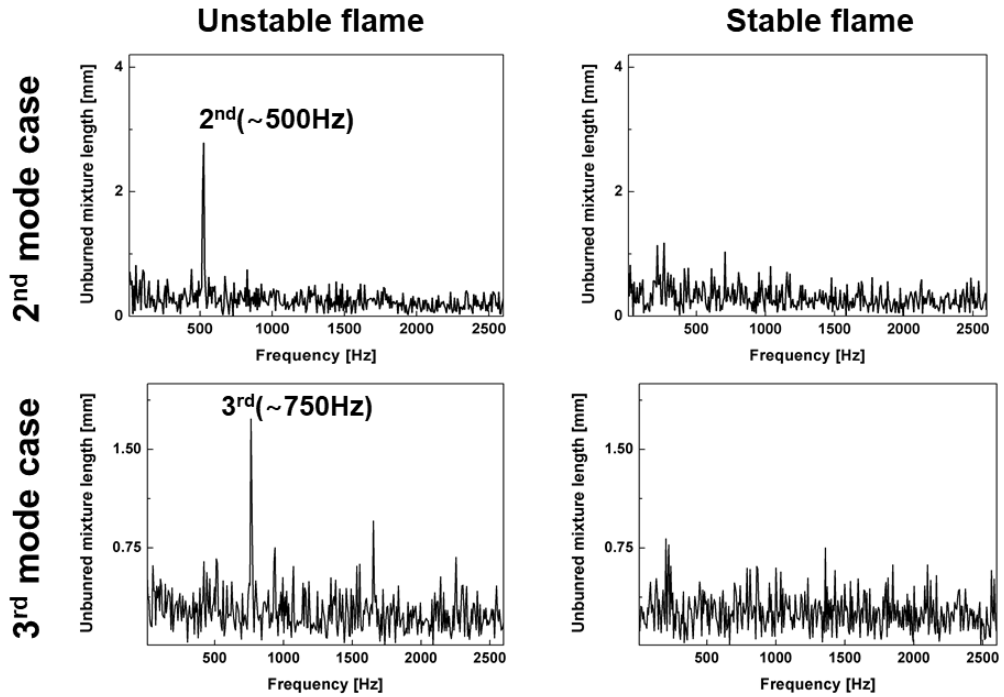


Figure 3.13 FFT results of the length of the unburned region in stable and unstable flames

In addition to confirming the length change frequency of the unburned region, the change tendency of the length of the unburned region in flame structure and the phase relation between dynamic pressure, heat release rate from OH chemiluminescence and length of the unburned region were also analyzed. Analysis of the 2nd mode case and the 3rd mode are presented in fig 3.14 and fig 3.15.

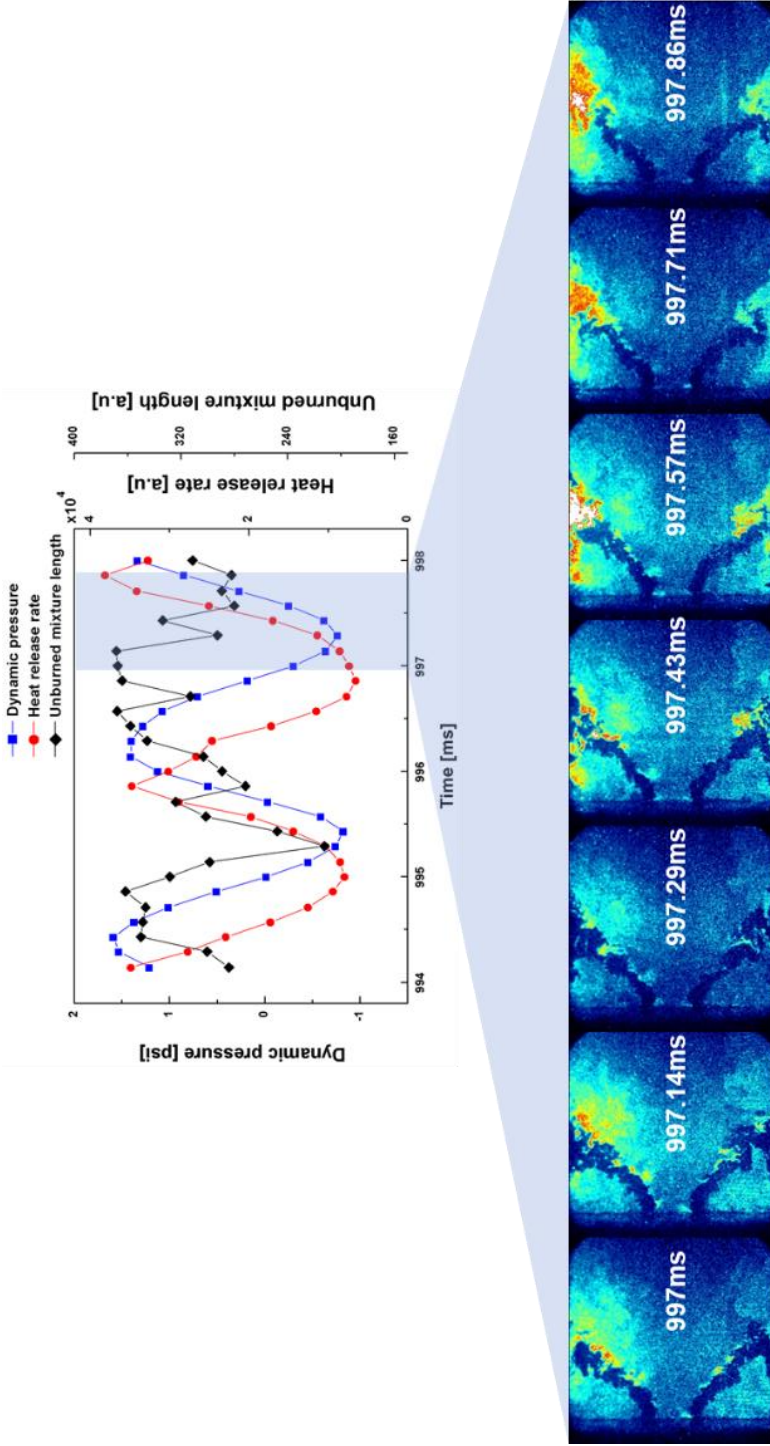


Figure 3.14 Change tendency of the unburned region and phase relation between p' , q' and the length of the unburned region of the 2nd mode case

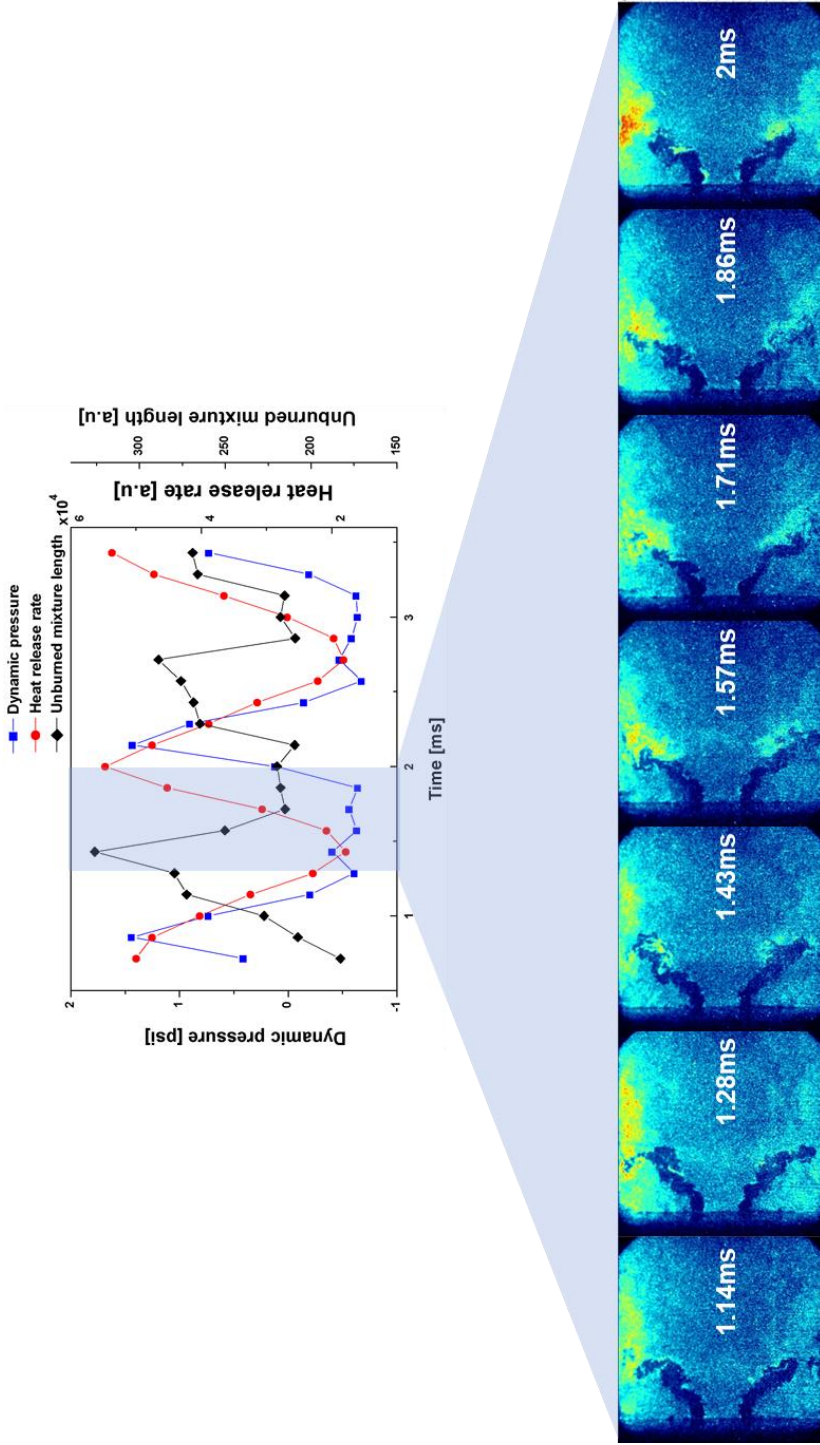


Figure 3.15 Change tendency of the unburned region and phase relation between p' , q' and the length of the unburned region of the 3rd mode case

The phase relation, that the change in dynamic pressure precedes to the change of the length of the unburned region, which precedes to change of heat release rate, is commonly confirmed in both 2nd mode and 3rd mode cases.

At the 2nd mode case, it can be found that lengthened unburned region becomes shorter as time passes, and relatively strong heat release rate is emitted when the length of the unburned region is shortened.

At the last case, it was confirmed that the length of the unburned region is relatively shorter than that of the prior case due to higher equivalence ratio. And same change tendency of flame structure was also appeared.

In addition to effect of small scale variation of flow rate on flame structure, effect on instability frequency was also investigated. As described above, when combustion instability occurs, small change of flow rate due to pressure fluctuation affects the mixing process of fuel and air. Therefore, when combustion instability occurs, the time required for complete mixing for fuel and air varied in partially premixed flame. However, fully premixed flame does not require time for mixing of fuel and air. As a result, the partially premixed flame have longer time for combustion than the fully premixed flame.

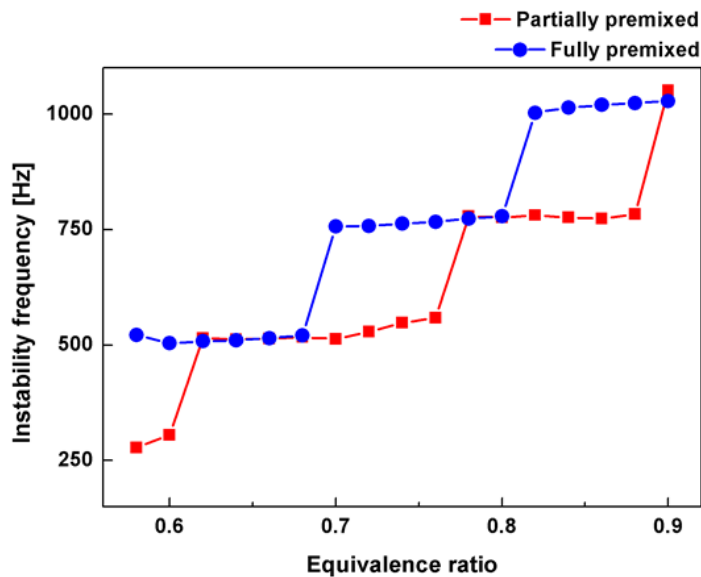


Figure 3.16 Instability frequencies of fully premixed flame and partially premixed flame varying equivalence ratio

The frequency of the combustion instability was observed while varying equivalence ratio from 0.58 to 0.9 under 1100 slpm of air flow rate in both fully premixed flame and partially premixed flame. The instability frequencies of fully premixed flame and partially premixed flame are presented in fig 3.16. Due to longer required time for combustion, the partially premixed flame had lower instability frequency compared to that of the fully premixed flame.

Flame structural difference between partially premixed flame and fully premixed flame was also analyzed at two equivalence ratio conditions (0.7, 0.82) which have different instability frequency. Averaged OH chemiluminescence images of the partially premixed flames and the fully premixed flames are presented in fig 3.17. An ignition delay time, that time for fuel-air mixture to be heated up to auto-ignition temperature, does not change according to equivalence ratio under fully premixed condition and this phenomenon was verified previous study [10]. Therefore, unlike fully premixed flames, which have an almost constant delay time required for combustion, the delay time of partially premixed flames for combustion varies as time goes. As a result, the change of position of partially premixed flames is larger than that of the fully premixed flames and because of this effect; partially premixed

flames have more similar to V-shape flame structure than fully premixed flames.

This structural difference also found in fig 3.17.

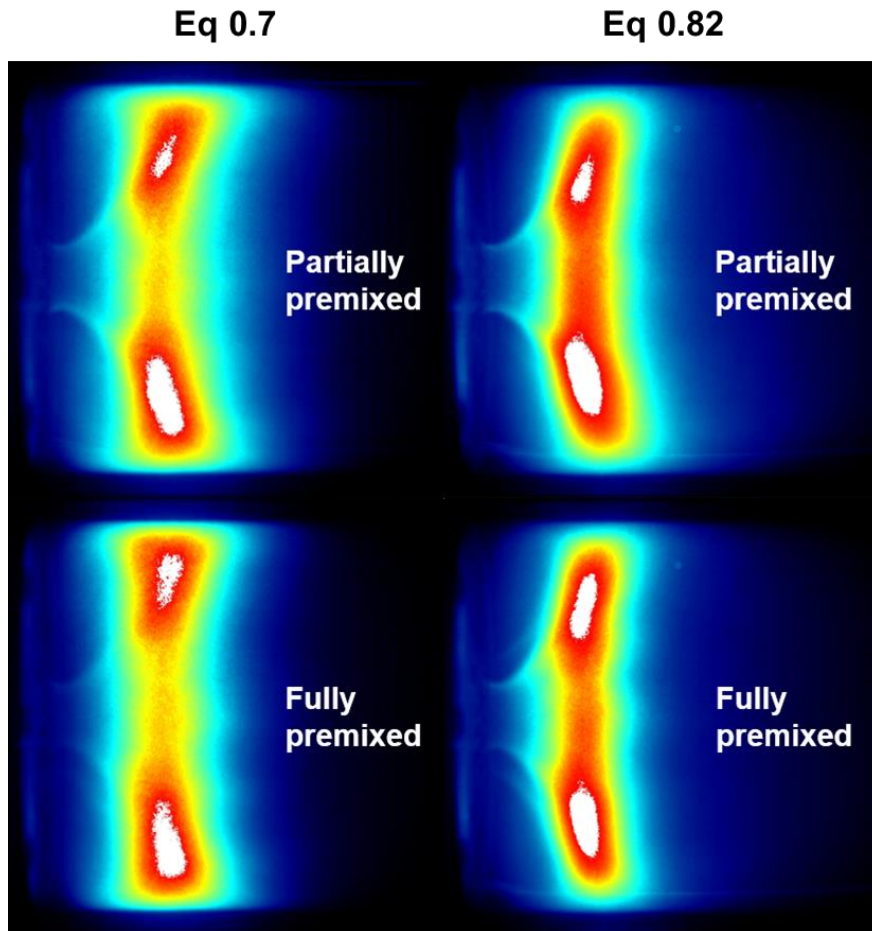


Figure 3.17 Averaged OH chemiluminescence images of partially and fully premixed flames at two different equivalence ratio conditions (0.7, 0.82).

Chapter 4 CONCLUSION

Effect of the flow rate change on the combustion instability in the partially premixed gas turbine combustor was investigated experimentally. The influence of the flow rate change was divided into effect of the large-scale variation and effect of the small-scale variation.

The experiments were divided into three conditions to confirm the effect of the large-scale flow rate variation. First, the fuel flow rate was increased while maintaining the air flow rate, thereby increasing the equivalence ratio. It could be found that the frequency of the combustion instability increased as the equivalence ratio increases. In this case, the position of the flame moved toward the dump plane, but the injection velocity after the nozzle was almost constant due to rarely increased total flow rate of the fuel-air mixture as the equivalence ratio increases. Therefore, the shortened convective delay time influenced increasing instability frequency.

Second, the air flow rate decreased while keeping the fuel flow rate, thereby increasing the equivalence ratio. In this case, unlike previous case, instability frequency did not change much in spite of the increased equivalence ratio. At this time, as the equivalence ratio increases, the flame moved toward to the dump plane

and the injection velocity also decreased. So, it had little effect on the convective delay time and the frequency of the combustion instability was almost constant.

Lastly, the effect of the increased total flow rate under constant equivalence ratio was also analyzed and it could be confirmed that the instability frequency increased as the flow rate increases. The flame position was kept almost constant at the same equivalence ratio in spite of increased total flow rate, but injection velocity increased inevitably due to increased total flow rate. As a result, it played a role of decreasing the convective delay time, resulting in an increase of the frequency of the combustion instability.

At the second part of this study, the effect of the small-scale flow rate change on the flame structure and frequency of the combustion instability was also analyzed. When combustion instability occurs, pressure in combustor fluctuates strongly and it causes the flow rate change at the injection nozzle. Modified injection velocity of fuel and air due to influenced flow rate by pressure fluctuation alters the degree of the fuel-air mixing. Because of the altered degree of mixing, when combustion instability occurred, the length of the unburned region had cyclic variation. Also, partially premixed flame have additional delay time, that fuel-air mixing process demand certain time, compared to fully premixed flame. So, the frequency of

partially premixed flame was normally lower than that of fully premixed flame due to relatively long delay time between pressure fluctuation and heat release rate oscillation.

Bibliography

- [1] T. C. Lieuwen and V. Yang, "Combustion instabilities in Gas Turbine Engines: Operational Experience, Fundamental Mechanisms, and Modeling", *AIAA*, 2006
- [2] Docquier. N. and Candel, S., "Combustion Control and Sensors: A Review", *Progress in Energy and Combustion Science*, 2002
- [3] T, Lieuwen, H. Torres, C. Johnson, B. T. Zinn, "A mechanism of combustion instability in lean premixed gas turbine combustor.", *J. Eng. Gas Turbines Power* , 2012
- [4] Sebastien, Ducruix., Thierry, Schuller., Daniel, Durox., and Sebastien, Candel. "Combustion dynamics and instabilities: Elementary coupling and driving mechanisms." *Journal of propulsion and power*, 2003
- [5] R. Balachandran, S. R. Chakravarthy, and R. I. Sujith, "Charaterization of an acoustically self-excited combustor for spray evaporation", *Journal of propulsion and power*, 2008
- [6] Yoon, J., Joo, S., Kim, J., Lee, M. C., Lee, J. G., and Yoon, Y. "Effects of convection time on the high harmonic combustion instability in a partially premixed combustor." *Proceedings of the Combustion Institute*, 2017

- [7] Lee, M. C., Ph.D thesis, *Seoul National Univ*, 2014
- [8] S. Taamallah, Z. A. Labry, S. J. Shanbhogue, M. A. Habib and A. F. Ghoniem, “Correspondence between “stable” flame macrostructure and thermos-acoustic instability in premixed swirl-stabilised turbulent combustion”, *J. Eng. Gas Turbines Power* , 2015
- [9] A.M. Kypraiou, P.M. Allison, A. Giusti and E. Mastorakos, “Response of flames with different degrees of premixedness to acoustic oscillations”, *Combustion Science and Tech.*, 2018
- [10] M. Brower, E. L. Petersen, W. Metcalfe, H. J. Curran, M. Furo, G. Bourque, N. Aluri, and F. Guthe, “Ignition delay time and laminar flame speed calculations for natural gas/hydrogen blends at elevated pressure”, 135(2), 2012

초 록

최근 지구온난화로 인한 환경문제가 대두됨에 따라, 가스터빈 산업계에 서는 NO, CO 등 배기가스를 줄이기 위한 많은 노력을 기울이고 있다. 가스터빈에서 배기가스를 줄이기 위해 가장 많이 사용하는 방법이 희박 예혼합방식의 연소방식이다. 하지만 희박예혼합연소 방식은 배기가스를 줄일 수 있다는 장점이 존재하지만 가스터빈의 하드웨어에 데미지를 주거나 작동 안정성에 영향을 줄 수 있는 연소불안정이 발생하기 쉽다는 단점이 존재한다. 따라서 가스터빈에서의 연소불안정 현상에 대한 많은 연구들이 진행되고 있다. 본 연구에서는 부분예혼합 가스터빈 연소기에서 연료와 공기 유량의 변화가 연소불안정 현상에 어떠한 영향을 주는지 OH-PLIF, PIV 와 같은 레이저 계측 방법을 통해 확인해보았다. 큰 폭으로 연료와 공기의 유량을 바꾼 경우에는 연소불안정 주파수가 낮은 주파수에서 높은 주파수로 변하는 현상이 확인되었고, 이 현상을 설명하기 위해 노즐로부터 화염까지의 거리를 혼합기의 분사속도로 나눈 convective delay time 의 개념을 도입하여 설명하였다. 여러 당량비, 평균유속 조건에서 실험을 진행하였고, convective delay time 의 감소와 연소불안정 주파수의 변화를 연관지어 설명하였다. 또한 노즐에서의 작

은 스케일의 유량 변화에 대한 영향도 관찰하였다. 연소불안정으로 인한 연소실 내부의 동압으로 인해 노즐에서는 연료와 공기의 미세한 유량변화가 발생하게 된다. 이때 유량변화로 인한 분사속도의 변화는 jet in crossflow 에서의 momentum ratio 를 변화시키게 되어 연료와 공기가 혼합되어 섞이는 정도를 바꾸게 된다. 따라서 유속변화로 인한 주기적인 연료와 공기 혼합의 정도의 변화는 미연소 영역의 길이의 변화로 이어지는 화염의 구조적인 특징을 확인할 수 있었다. 또한 부분예혼합화염의 경우, 예혼합화염과는 달리 연료와 공기가 섞이는데 필요한 추가적인 시간이 존재하기 때문에 상대적으로 압력 섭동과 열방출량 섭동 사이의 시간 차이가 더 크기 때문에 예혼합화염에 비해 낮은 연소불안정주파수를 가지는 것을 확인할 수 있었고, 연료와 공기가 섞이는데 필요한 시간이 주기적으로 변화하기 때문에 예혼합화염에 비해 화염의 위치변화가 커, 상대적으로 V 형태에 더 가까운 화염의 구조를 가지는 것 또한 확인할 수 있었다.

주요어 : 가스터빈 연소기, 연소불안정, 화염 구조, 불안정 주파수 천이
현상

학번 : 2017-28315